OBSERVATIONS OF FATIGUE CRACK INITIATION AND DAMAGE GROWTH IN NOTCHED TITANIUM MATRIX COMPOSITES

R. A. Naik and W. S. Johnson

January 1990

OBSERVATIONS OF FATIGUE CRACK INITIATION AND DAMAGE GROWTH

IN NOTCHED TITANIUM MATRIX COMPOSITES

R. A. Naik[*] and W. S. Johnson

NASA Langley Research Center

Hampton, VA.

ABSTRACT

The purpose of this study was to characterize damage initiation and growth in notched titanium matrix composites at room temperature. Double edge notched or center open hole SCS-6/ Ti-15-3 specimens containing 0° plies or containing both 0° and 90° plies were fatigued. The specimens were tested in the as-fabricated (ASF) and in heat-treated conditions. A local strain criterion using unnotched specimen fatigue data was successful in predicting fatigue damage initiation. The initiation stress level was accurately predicted for both a double edge notched unidirectional specimen and a cross-plied center hole specimen. The fatigue produced long multiple cracks growing from the notches. These fatigue cracks were only in the matrix material and did not break the fibers in their path. The combination of matrix cracking and fiber/matrix debonding appears to greatly reduce the stress concentration around the notches. The laminates

[*]Analytical Services and Materials, Inc., Hampton, Virginia.

that were heat treated showed a different crack growth pattern. In the ASF specimens, matrix cracks had a more torturous path and showed considerably more crack branching. For the same specimen geometry and cyclic stress, the [0/90/0] laminate with a hole had far superior fatigue resistance than the matrix only specimen with a hole.

KEYWORDS: Metal matrix composite, silicon carbide fibers, fiber/matrix interface.

INTRODUCTION

Titanium metal matrix composites (MMC) are being considered for high temperature structural applications on man-rated aircraft. Prior to application, however, the fatigue and damage tolerance behavior of these materials must be well understood and be predictable. The purpose of this paper is to present an analytical and experimental study that describes some details of the fatigue crack initiation and growth in specimens containing either a crack-like slit or a circular hole. This study follows previous work on the unnotched, room-temperature behavior of titanium/ silicon carbide composites [1] and on the effect of a high temperature cycle on the mechanical behavior of this composite [2]. A brief review of the pertinent unnotched fatigue data from the previous reports will be given in the following section. This will be followed by a description of the material and specimens and the testing procedures used. Then the predicted damage initiation stress levels are compared to those observed experimentally. In addition, micrographs will show the crack growth progression as a function of applied load cycles. In some cases the

surface crack growth is compared to etched or polished specimens which reveal the subsurface damage in the matrix and fiber. Some rationale for the observed damage growth will be discussed.

BACKGROUND

Data for the applied maximum cyclic stress versus the number of load cycles to failure was presented for four lay-ups of SCS-6/Ti-15-3 in reference [1]. The room temperature data for the as-fabricated specimens is shown in Figure 1. All of the lay-ups, $[0]_8$, $[0_2/\pm45]_2$, $[0/\pm45/90]_2$, and $[0/90]_{2s}$, contain 0^0 plies. Since the fiber/matrix interfaces in the off-axis plies fail after a very few cycles [1], the 0^0 plies carry most of the load during the fatigue life of these specimens. Because of these interface failures in the off-axis plies, those laminates containing off-axis plies experience a significant reduction in overall stiffness in the first few cycles. After the first few cycles, however, the stiffness remains constant for the remainder of the fatigue life until just prior to specimen failure. The strain range is, therefore, also constant with the applied constant loading after the first few cycles. This strain range can be multiplied by the fiber modulus of 400 GPa to yield the cyclic stress in the 0^0 fiber during essentially the entire fatigue life [1]. When the cyclic stress in the 0^0 fibers was calculated for each data point in Figure 1 and plotted against the number of cycles to fatigue failure, the data from the four different laminates collapsed into a narrow band, as shown in Figure 2. This suggests that the fatigue life of a given laminate is a function of the stress in the 0^0 fiber. This is reasonable since none of the laminates tested will fail until the 0^0 plies fail. The cycles to failure as a function of the overall laminate strain range is also shown in

figure 2. This data, in terms of the strain range, will be used later to predict local damage using a strain range criterion.

Naik, Johnson and Pollock [2] have shown that the mechanical behavior of SCS-6/Ti-15-3 [0/90/0] laminate can be significantly effected by exposure to the high temperature cycle (described later) associated with a superplastic forming/diffusion bonding (SPF/DB) process. Figure 3 shows an S-N curve for the as-fabricated (ASF) and the SPF/DB materials. The data shows that the SPF/DB material experienced a 25 percent drop in static strength and a significant reduction in fatigue resistance. This degradation in mechanical behavior was attributed to a change in failure mode caused by an increase in the fiber/matrix interface strength and an increase in the thermal residual stresses in the matrix surrounding the fiber. Figure 4 shows a schematic of the failure processes described in [2]. In the ASF case, the interface was weak and the residual stresses were lower, thus, allowing the matrix crack to debond along the length of the fiber and then continue on the other side of the fiber without breaking the fiber. In the SPF/DB case, the interface strength was strong enough, coupled with the higher thermal residual stresses [2], to cause the matrix crack to propagate through the fibers. As described in [2], it can be shown by a shear lag analysis [3] that the stress in the first unbroken fiber in the crack path is 35 percent higher for the SPF/DB failure mode (figure 4), thus explaining the resulting change in mechanical behavior.

The present work will examine how fatigue damage initiates and grows in the presence of a stress concentration and the applicability of the knowledge of the failure process observed in an unnotched coupon to the local area at a notch tip.

4

EXPERIMENTAL PROCEDURES

Materials and Specimens

All specimens were made of SCS-6/Ti-15V-3Cr-3Al-3Sn (referred to as SCS-6/Ti-15-3). Ti-15-3 is a metastable beta titanium alloy [4]. SCS-6 fibers are silicon carbide fibers that have a carbon core and a thin carbon-rich surface layer [5]. The typical fiber diameter is 0.142 mm. The composite laminates are made by hot-pressing Ti-15-3 foils between unidirectional tapes of SCS-6 fibers. The layups used in the present study were $[0]_8$, $[0/90]_{2s}$, and $[0/90/0]$. The thickness of the 8-ply and 3-ply specimens was approximately 2 mm and 0.68 mm, respectively. The fiber volume fractions for the 8-ply and 3-ply specimens were approximately 0.325 and 0.375, respectively.

All specimens were 19-mm wide and about 140-mm long and were cut using a diamond wheel saw. As shown in Fig. 5(a), the $[0]_8$ specimens were machined using electro-discharge machining with edge notches that were 0.45 mm thick and 3 mm long. The $[0/90]_{2s}$ and $[0/90/0]$ specimens had center holes that were machined using a diamond core drill and were 6.35 mm in diameter (Fig. 5(b)).

All 8-ply specimens were tested in the as-fabricated (ASF) condition, except one unidirectional edge notched specimen, which was in the aged condition. This ageing was conducted at 482°C for 16 hours. As discussed in reference [1], this ageing had a significant effect on the properties of the Ti-15-3 material and also increased the fiber/matrix interface strength.

The $[0/90/0]$ specimens were cut from two panels. One of the panels was in the as-fabricated (ASF) condition. The second panel was subjected

5

to a thermal processing cycle that simulated a superplastic forming/ diffusion bonding (SPF/DB) operation. This simulated SPF/DB cycle was performed in a vacuum furnace and consisted of raising the temperature from ambient to 700°C at a rate of 10°C per minute. After stabilizing at 700°C the temperature was further increased to 1000°C at a rate of 4°C per minute. The panel was held at 1000°C for 1 hour. It was then furnace cooled to 594°C at a rate of 8°C per minute and held at that temperature for 8 hours. Finally, it was furnace cooled to 150°C and held for about 10 hours before cooling down to ambient temperature. As described in reference [2], in the unnotched laminates, this SPF/DB cycle increases the thermal residual stresses in the composite and also leads to an increased fiber/matrix interface strength.

One rectangular unreinforced titanium specimen (19 mm by 140 mm) with a center hole (6.35-mm diameter) was also tested. This unreinforced titanium specimen was a "fiberless composite" made by consolidating Ti-15-3 foils with the same temperature-time-pressure cycle used for the composite laminates.

Test Procedure and Equipment

The specimens were tested in a hydraulically-actuated, closed-loop, servo-controlled testing machine. The load, measured by a conventional load cell, was used for the feedback signal. All specimens were tested under constant amplitude fatigue at a frequency of 10 Hz and a stress ratio R of 0.1. Two different test approaches were used in the present study. To study damage initiation, some specimens were tested using an incremental loading approach. Thus, the $[0]_8$ and $[0/90]_{2s}$ ASF specimens, edge notched and center hole, were tested at a series of stress range values; at each

stress range they were tested for 50,000 cycles before the stress range was increased (see Table 1). To study damage growth, other specimens were tested at a constant stress range. Thus, the aged $[0]_8$ specimen and the [0/90/0] ASF and SPF/DB specimens were tested at a constant stress range.

The fatigue tests were stopped periodically and the specimens were radiographed at 75 percent of the maximum cyclic stress with an industrial-type "soft" X-ray machine with a 0.25-mm thick beryllium window and a tungsten target. The voltage was set at 50 kV for the $[0]_8$ and $[0/90]_{2s}$ specimens and at 40 kV for the [0/90/0] specimens. A Kodak high resolution X-ray film (type M-II) was mounted to the specimen on the opposite side. The X-ray target-to-film distance was 610 mm. The [0/90/0] specimens were exposed at 5 mA for 75 s, while the other specimens were exposed at 20 mA for 60 s. This procedure resulted in good contrast between the fibers and the matrix (see figure 6). A thin aluminum plate, 0.7-mm thick, was used as a filter and placed between the specimen and the X-ray tube. This resulted in good definition along the edges of the hole and the notches. Along with the X-rays, surface replicas and clip gage readings were also taken periodically.

Before testing the specimens, the region around the hole and the notches was polished by fine grain sandpaper to aid visual observations of fatigue damage initiation and growth. The polished surfaces also helped in getting good quality replicas of the damage around the hole and the notches. Cellulose acetate film was used to make surface replicas at various stages of crack initiation and growth. The replicas were then studied under an optical microscope. For the open hole specimens, a clip gage, located diametrically inside the hole, was used to record load versus hole elongation (along the loading direction) at various stages of

undamaged and damaged specimen history. Such a local load-elongation plot would show a marked change in the local stiffness if there were any fiber failures associated with the visible surface cracks.

After testing, some specimens were sectioned and polished to study the internal damage in the matrix and the fibers. Other specimens were exposed to hydroflouric acid to dissolve the surface layer of titanium to expose the fibers beneath.

RESULTS AND DISCUSSION

Test results and discussions for the double edge notched specimens are first presented for both the ASF and the aged specimens. These are followed by a description of the results for the $[0/90]_{2s}$ ASF and the [0/90/0] ASF and SPF/DB center-hole specimens. Finally, results for the center open hole "fiberless matrix" specimen are presented.

Double Edge Notched Specimens

Both the ASF and aged specimens were tested in the double edge notched configuration. As mentioned, the $[0]_8$ ASF specimens were tested using an incremental stress range approach in which the specimen was fatigued at each stress range for 50,000 cycles (see Table 1). The objective of using such an incremental approach was to determine the stress range at which damage initiation occurred. It was important to make a reasonable prediction of the damage initiation stress before starting the test. The data in figure 2 for unnotched SCS-6/Ti-15-3 laminates was used together with the computed notch stress concentration factor to make such a prediction. According to the data in figure 2, the unnotched $[0]_8$ laminate

has an endurance strain range (at 50,000 cycles) of 0.0033. Using the computed stress concentration factor of 5.61 for the notched laminate (see Appendix), it can be shown, using a simple rule of mixtures analysis, that an applied maximum cyclic stress of 122 MPa would result in local damage initiation after 50,000 cycles for the notched laminate. For the ASF specimen, tested using the incremental stress range approach, damage initiation was observed after 25,000 cycles at a maximum cyclic stress of 122 MPa (see Table 1). Also, a second ASF specimen (see Table 1) was tested using the incremental stress range approach starting at a cyclic maximum stress of 250 MPa. Using the rule of mixtures and the computed stress concentration of 5.61 this will lead to a local strain range of 0.006 at the notch tip. According to the data in figure 2, local damage initiation would occur at this strain range after 5000 cycles. Damage initiated in this specimen after 7,500 cycles at a maximum cyclic stress of 250 MPa. The same incremental stress range approach was continued after damage initiation in order to study damage growth in these specimens. In contrast to the test procedure for the ASF specimens, the aged specimen was tested at a constant stress range the entire test in order to study fatigue damage growth.

Figure 7 shows micrographs of surface replicas of the regions near the notch tips for an $[0]_8$ ASF specimen (see Table 1 for load history). All replicas were taken after 50,000 cycles at a particular maximum cyclic stress. Figure 7(a) shows damage growth in its early stages. Cracks start to grow from the corners of the notches at about 45 degrees to the fiber direction. At higher loads, secondary cracks initiate from the notches and grow at angles approaching the fiber direction (figure 7(b) and 7(c)). There is also evidence of crack branching. The first 45 degree cracks

change direction and tend to grow in a direction perpendicular to the fiber

direction. At still higher loads (figure 7(d)), the secondary cracks

become the dominant cracks and start growing almost parallel to the fiber

direction. Again, there is more evidence of crack branching.

In order to ascertain whether fiber failure was associated with the

surface cracking seen in figure 7, some specimens were treated with

hydroflouric acid after testing. This treatment dissolved the titanium

from the surface. The acid first seeped into the surface cracks and, thus,

etched deeper in those regions where there were surface matrix cracks.

This led to the fibers being more clearly visible in these regions. Such

preferential etching of the surface layer allowed to preserve the original

cracking pattern, to some extent, while exposing the fibers directly

beneath the surface cracks. Figure 8 shows micrographs of an acid-etched

specimen along with photographs of replicas showing corresponding surface

damage. All of the fibers underneath the surface cracks appear to be

intact. The absence of fiber failure was also confirmed by the

radiographs.

The aged $[0]_8$ specimen showed significant differences in the damage

growth patterns from the notch tips. As shown by the photographs of

surface replicas in figure 9, the cracks initiate at 45 degrees to the

fiber direction. However, unlike the ASF specimens, there are no secondary

cracks and the 45 degree cracks are the dominant cracks. After about

100,000 cycles these 45 degree cracks change direction and continue growing

perpendicular to the fiber direction. For the specimen shown in figure 9,

one of the cracks started in a direction almost perpendicular to the fiber

direction and then branched into two 45 degree cracks. This growth may

have been due to a broken fiber that was found ahead of the notch, which

could force the matrix to crack at that point. This fiber could have been broken by the machining process.

Figure 10 shows micrographs of the aged $[0]_8$ specimen before and after it was treated with hydroflouric acid. All of the fibers underneath the surface cracks appear to be intact. There is only one broken fiber visible next to one notch and, as mentioned above, this could have been the result of the notch machining process.

The most significant finding in the above tests, on both the ASF and aged $[0]_8$ notched specimens, was that the cracks grew only in the matrix leaving the fibers intact. The test stress levels were chosen by considering the stress concentration of the notch and the strain range at which fatigue failure had been observed for the unnotched laminate (Figure 2). It was expected that the matrix cracking would preceed fiber breakage only by a short distance. The lack of fiber failure suggests that the multiple matrix cracking and/or fiber/matrix debonding led to a reduction of the notch stress concentration to a level that was below the fatigue endurance limit of 1320 MPa for the SCS-6 fibers (see Figure 2).

The initiation of matrix cracks at 45^0 to the fiber direction, in both the ASF and aged $[0]_8$ specimens, was another unexpected finding. According to the finite element analysis (see Appendix) of the notched specimen, the critical region for crack initiation lies along a line joining the two edge notches and not along a 45^0 line from the notches. One explanation for the 45^0 cracks could be the presence of fiber/matrix debonding at the fiber next to the notch. According to the micromechanics analysis in reference 7, there are high tensile stresses acting normal to fiber just ahead of the notch. These stresses could lead to fiber/matrix debonding before the cyclic load cracks the matrix. A debond in the

11

fiber/matrix interface just ahead of the notch tip will redistribute the stresses locally causing a shift in the critical crack initiation region to be along a 45° line instead of along the net section.

Center Hole Specimens

Center hole specimens made from an ASF $[0/90]_{2s}$ laminate and ASF and SPF/DB [0/90/0] laminates were also tested in the present study. The $[0/90]_{2s}$ ASF specimen was tested using the same incremental approach used for edge notched specimens. The [0/90/0] specimens were tested at a constant stress range in order to study damage growth and have a direct comparison of the cracking behavior of the ASF to the SPF/DB condition.

The data in figure 2 for unnotched SCS-6/Ti-15-3 laminates was used together with the computed hole stress concentration factor (see Appendix) and AGLPLY [6] to make a prediction of the damage initiation stress before starting the incremental stress testing. According to the data in figure 2, the unnotched $[0/90]_{2s}$ laminate would have a fatigue endurance limit at a laminate strain range of 0.0033. Using the computed stress concentration factor of 3.60 (see Appendix) for the center hole $[0/90]_{2s}$ laminate [8], it was shown that an applied maximum cyclic stress of 160 MPa would result in local damage initiation after 50,000 cycles for the $[0/90]_{2s}$ center hole laminate. Testing was started at a maximum cyclic stress of 137 MPa (see Table 1). For the $[0/90]_{2s}$ specimen tested using the incremental approach, damage initiation was observed after 1000 cycles at a maximum cyclic stress of 150 MPa. The same incremental stress range approach was continued after damage initiation in order to study damage growth in this specimen. The [0/90/0] ASF and SPF/DB specimens were tested at a constant maximum cyclic stress of 215 MPa which corresponds to a local maximum cyclic stress of 780

12

MPa using a stress concentration factor of 3.62 at the hole. From Figure 3 this stress level should have resulted in local damage in 17,000 cycles for the ASF specimen and 100 cycles for the SPF/DB. For the ASF specimen tested damage initiation was observed at 50,000 cycles and at 40,000 cycles for the SPF/DB specimen.

Figure 11 shows a photograph of the multiple crack pattern that was observed in the center-hole $[0/90]_{2s}$ specimen. The cracks are the light streaks seen in the photograph. This type of damage was also observed by Harmon and Saff [9] for center hole specimens of SCS-6/Ti-15-3. In order to study the internal damage, the specimen shown in figure 11 was sectioned and polished. Figure 12 shows micrographs of the damage in the 0° ply. Figure 12(a) shows cracks in the matrix but no fiber failure. Figure 12(b) shows a close-up view of one of these matrix cracks and the region around it. There is evidence of fiber/matrix debonding along the first fiber next to the hole and also on both sides of the matrix cracks. This corresponds to the ASF failure mechanism shown in figure 4.

Figure 13 shows micrographs of surface replicas for an ASF [0/90/0] specimen. There is evidence of multiple matrix cracking similar to that seen in the double edge notched ASF specimens. There is also a tendency for crack branching. After about 1,000,000 cycles, the cracks had grown to the edges of the specimen. However, based on the clip gage readings there was only a 8 percent difference in the local stiffness after 100,000 cycles. This suggests that the matrix cracks were not accompanied by fiber failure. This was confirmed by the radiographs and by etching away the surface layer of titanium.

Figure 14 shows fatigue damage growth for the SPF/DB [0/90/0] specimen. Multiple cracking around the hole boundary was observed as in

the ASF specimen. However, these cracks were straighter than those in the ASF specimen and showed no branching. Again, the clip gage readings showed only a 2.6 percent difference in the local stiffness (after 50,000 cycles), indicating a lack of fiber failure. This was confirmed by the radiographs and by etching away the surface layer of titanium.

The lack of fiber failure was once again the most unexpected finding for the center-hole specimens. The test stress levels were chosen by considering the stress concentration of the hole and the fatigue S-N curve of the unnotched laminate. The applied stress should have been high enough to fail the fibers next to the hole. Apparently the stress concentration at the hole was significantly reduced after a few cycles by a combination of matrix cracking and/or fiber/matrix debonding. For example, consider the ASF [0/90/0] specimen containing a center hole with a stress concentration factor of 3.62. The maximum local stress at the edge of the hole was estimated to be about 780 MPa for the applied maximum cyclic stress of 215 MPa. Based on the S-N curve for the ASF [0/90/0] specimen in Figure 3, local damage, including fiber failure, would be expected at approximately 17,000 cycles. However, the matrix cracks and the fiber/matrix debonding near the hole lowered the stress concentration. This was shown in Figure 12, for the $[0/90]_{2s}$ specimen, where the first fiber next to the hole has debonded from the matrix. Some theoretical estimates of the effect of this type of fiber/matrix debonding have been examined by Goree and Gross [3] using a shear-lag theory. If we assume that the fiber/matrix debonding effectively removed the stress concentration due to the hole, then the net section stress for the [0/90/0] ASF specimen would be 320 MPa (215 MPa/0.67, the ratio of net section to gross section area) for an applied maximum cyclic stress of 215 MPa.

14

Figure 3 shows that the 320 MPa stress is well below the fatigue limit for the ASF laminate. Even if the matrix were completely cracked in the net section and the fibers carried all the load, the stress in the 0° fibers would be 865 MPa (320 MPa/0.37, the fiber volume fraction). Figure 2 shows that this value of fiber stress is well below the fatigue limit for the fibers.

The limiting fiber stress range is approximately 1320 MPa (see Figure 2). This corresponds to a strain range in the fiber, and also in the composite, of 0.0033. Thus, the strain range in the [0/90/0] composite should be atleast 0.0033 in order to break fibers. Using a composite longitudinal modulus of 156 GPa [2], the maximum cyclic stress in the composite should be atleast 572 MPa in order to break fibers. Assuming the matrix carries its share of the load, the stress concentration would, therefore, have to be below 2.66 (computed as the ratio (572 MPa/215 MPa)) in order to not fatigue the fibers, next to the hole, beyond their fatigue limit. It does not seem unreasonable to think that local fiber/matrix debonding at the hole could lower the stress concentration from the original 3.62 to below 2.66. These results indicate that if the stress concentration is reduced (eg. by fiber/matrix debonding), a much higher laminate stress is required before the 0° fibers and, subsequently, the composite will fail.

Finally, an unreinforced titanium specimen was tested at the same stress range used for the [0/90/0] ASF and SPF/DB specimens. A crack initiated for this specimen at about 25,000 cycles and a single crack grew from each side of the hole along the net-section of the specimen. The specimen failed at 31,000 cycles when the fatigue crack on one side of the hole grew to the edge of the specimen. This indicates that the composite

is much more resistant to fatigue failure than the matrix alone. Although the matrix material of the composite showed significant fatigue cracks, the fibers acted to retain stiffness and to carry the load. The fact that the matrix cracks grew around the fibers without fracturing the fibers in the ASF [0/90/0] composite, even when the matrix cracks were quite long, is an interesting, and somewhat unexpected, phenomenon. Marshall, Cox and Evans [10] have discussed analytically how a long matrix crack can reach a steady state crack growth condition without failing fibers in a ceramic matrix composite.

CONCLUSIONS

The purpose of this study was to characterize damage initiation and growth in notched titanium matrix composites at room temperature. Double edge notched or center hole SCS-6/Ti-15-3 specimens containing either unidirectional plies or both 0° and 90° plies were fatigued. The specimens were tested in the as-fabricated (ASF) or in one of two heat-treated conditions. Replicas of the surface cracks were taken during the fatigue testing. Radiographs were also taken periodically during testing to monitor fiber breaks. Several of the specimens were either acid etched or polished to reveal subsurface damage. The following conclusions were derived from this investigation:

A local strain criterion using unnotched specimen fatigue data was successful in predicting fatigue damage initiation in the matrix. The initiation stress level was accurately predicted for both a unidirectional double edge notched specimen and a cross-plied center hole specimen.

The fatigue loading produced long multiple fatigue cracks growing from the notches. These fatigue cracks were only in the matrix material and did not break the fibers in their path.

The combination of matrix cracking and fiber/matrix debonding appears to greatly reduce the stress concentration around the notches.

The laminates that were heat treated (either aged or SPF/DB) showed fatigue behavior similar to the ASF specimens. However, the matrix cracks in the ASF specimen had a somewhat more torturous path and showed considerably more crack branching.

For the same notch geometry and cyclic stress, the [0/90/0] laminate had far superior fatigue resistance than the matrix material alone.

REFERENCES

1. Johnson, W. S., Lubowinski, S. J. and Highsmith, A. L.; "Mechanical Characterization of Unnotched SCS-6/Ti-15-3 Metal Matrix Composites at Room Temperature," To be published in Thermal and Mechanical Behavior of Ceramic and Metal Matrix Composites, ASTM STP 1080, Kennedy, Moeller, and Johnson, Ed., 1990.

2. Naik, R. A., Johnson, W. S., and Pollock, W. D.; "Effect of a High Temperature Cycle on the Mechanical Properties of Silicon Carbide/ Titanium Metal Matrix Composites," Proceedings of the American Society for Composites, Dayton, Ohio, 1989, pp. 94-103.

3. Goree, J. G. and Gross, R. S., "Analysis of a Unidirectional Composite Containing Broken Fibers and Matrix Damage," Engineering Fracture Mechanics, Vol. 13, pp. 563-578.

4. Rosenberg, H. W., "Ti-15-3: A New Cold-Formable Sheet Titanium Alloy," _Journal of Metals_, Vol. 35, No. 11, November 1986, pp. 30-34.

5. Wawner, F. E., Jr., "Boron and Silicon Carbide/ Carbon Fibers," Fibre Reinforcements for Composite Materials, Ed. A. R. Bunsell, 1988, Elsevier Science Publishers B. V., Amsterdam, The Netherlands.

6. Bahei-El-Din, Y. A. and Dvorak, G. J., "Plasticity Analysis of Laminated Composite Plates," ASME _Journal of Applied Mechanics_, Vol. 49, 1982, pp. 740-746.

7. Chai, L., and Dharani, L. R., "A Micromechanics Model for Prediction of Failure Modes in Ceramic Matrix Composites," Final Report NASA Contract No. NA53-25333, August 1988.

8. Harmon, D. M., Saff, C. R., and Sun, C. T., "Durability of Continuous Fiber Reinforced Metal Matrix Composites," AFWAL-TR-87-3060, October 1987.

9. Harmon, D. M. and Saff, C. R., "Damage Growth in Fiber Reinforced Metal Matrix Composites," _Metal Matrix Composites: Testing, Analysis and Failure Modes, ASTM STP 1032_, W. S. Johnson, Ed., American Society for Testing and Materials, Philadelphia, 1989.

10. Marshall, D. B., Cox, B. N., and Evans, A. G., "The Mechanics of Matrix Cracking in Brittle Matrix Composites," _Acta Metallurgica_, Vol. 33, No. 11, pp. 2013-2021, 1985.

APPENDIX

The stress concentration factors for the edge-notched specimens and the center-hole specimens were determined by two different techniques. In both cases, the specimen was assumed to be an orthotropic laminate and the

corresponding laminate properties were obtained by using AGLPLY [6] and the fiber and matrix properties from reference [1].

The edge-notched specimens were analyzed using a two dimensional finite element analysis. Isoparametric, quadrilateral elements were used with a very fine mesh refinement next to the notch. A convergence study for the mesh refinement was conducted by comparing the computed stress concentration factor for an isotropic specimen with handbook values.

The center-hole specimens were analyzed using the equations in reference [8] for orthotropic laminates. The effects of finite width on the stress concentration are also appropriately accounted for by the equations in reference [8].

Table 1:- Test matrix and loading history (at R — 0.1) for the specimens tested.

Specimen Type	Figure(s)	Cycles	Maximum Cyclic Stress (MPa)
Edge Notched Specimens			
ASF, $[0]_8$	8	50,000	122^a,133,148,163,180,198,215, 239,262,290,315,350,383
ASF, $[0]_8$	7	50,000	250^a,280,310,345,380,422
Aged, $[0]_8$	9,10	850,000	250
Center Hole Specimens			
ASF, $[0/90]_{2s}$	11,12	50,000	137, followed by,
		70,000	150
ASF, [0/90/0]	13	4,000,000	215
SPF/DB, [0/90/0]	14	2,680,000	215
ASF Matrix, Ti-15-3	--	$31,000^b$	215

[a] Specimens were tested at each of the maximum cyclic stresses (at R — 0.1) for 50,000 cycles in the order in which they are listed.

[b] Only case where fatigue failure was observed; all other specimens did not fail after the completion of the loading history above.
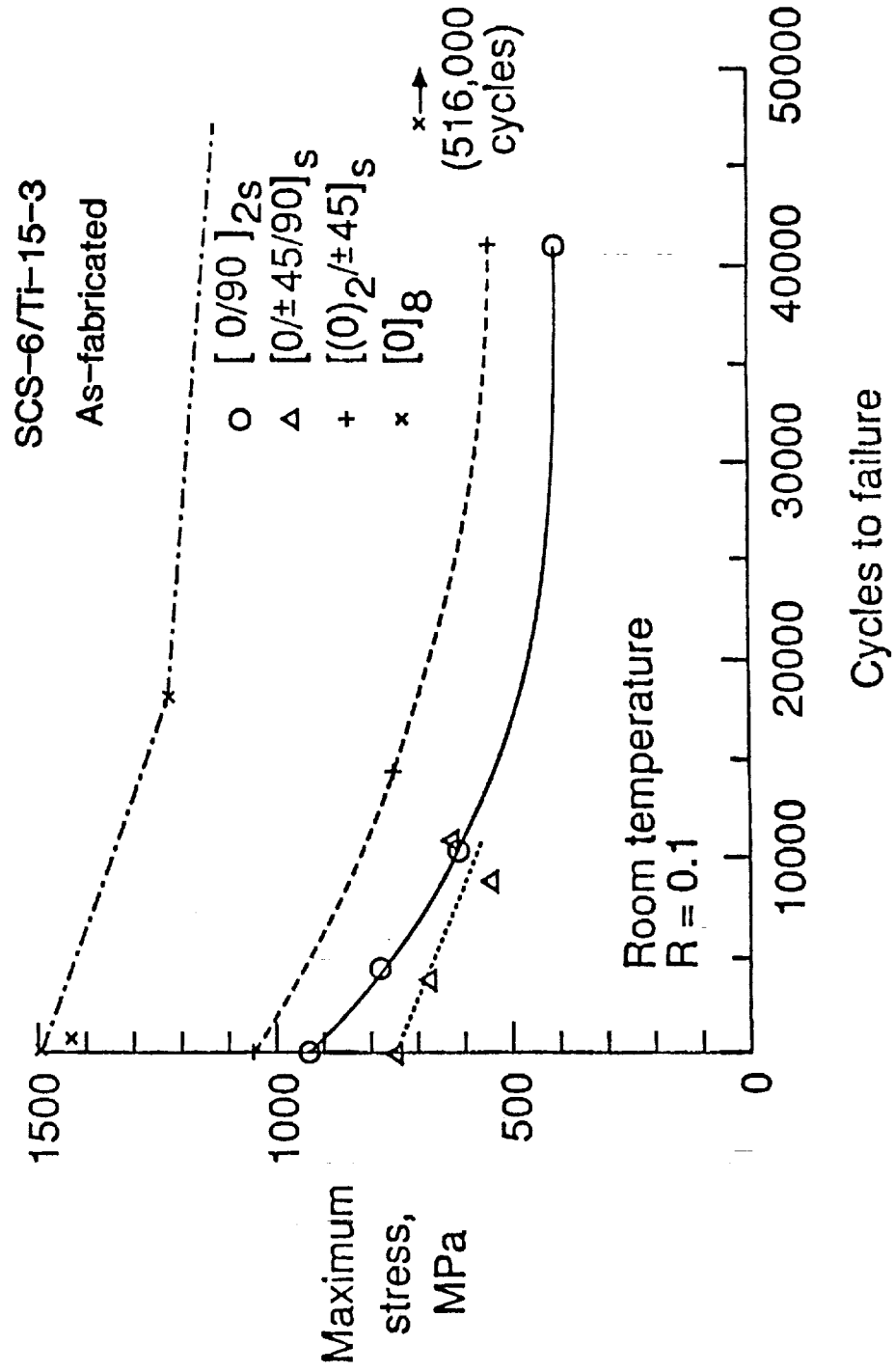
Figure 1.- S-N curves for SCS-6/Ti-15-3 laminates [1].
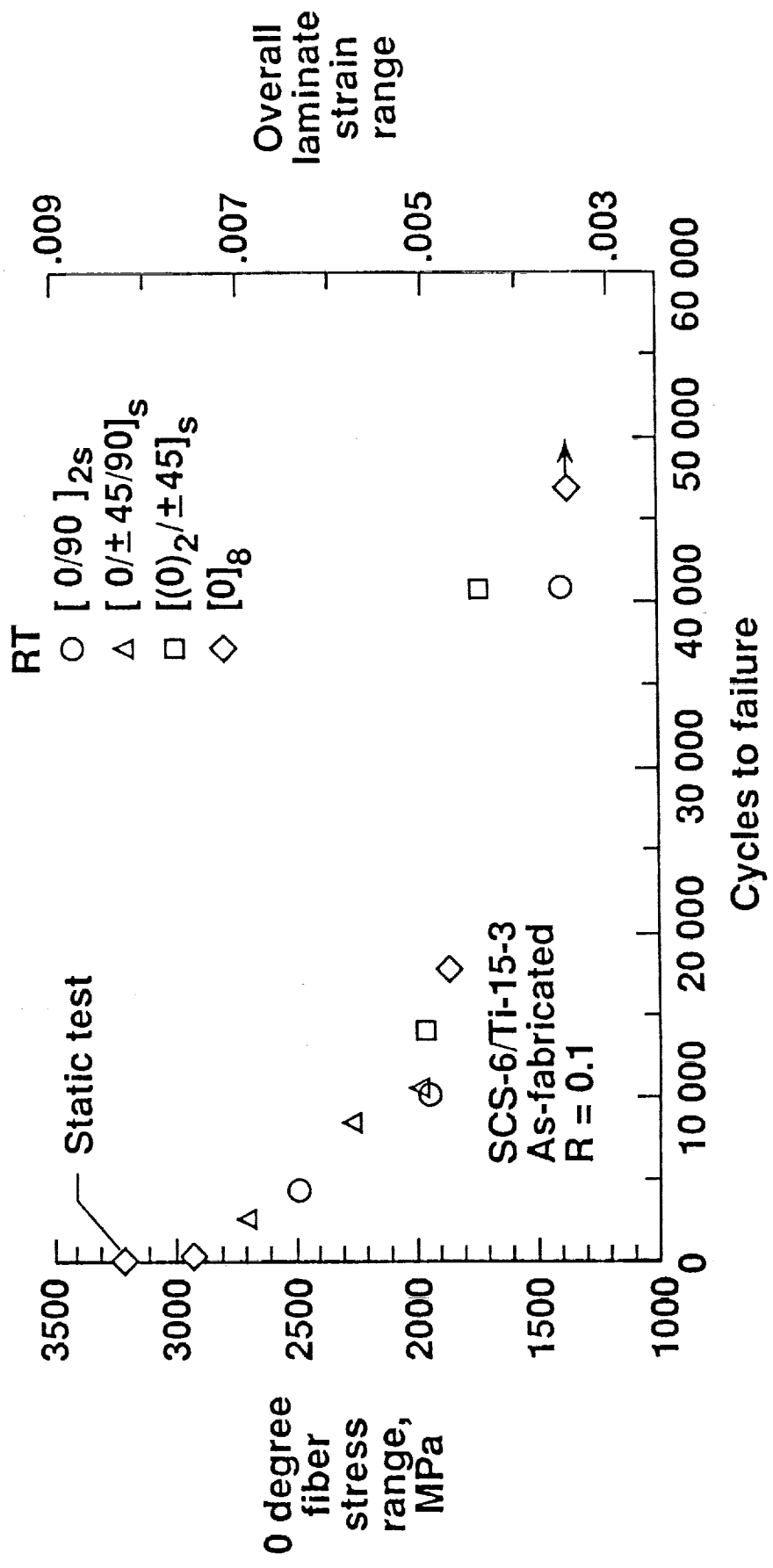
Figure 2.- Cyclic stress range in $0°$ fiber and laminate strain range versus number of cycles to laminate failure[1].

22
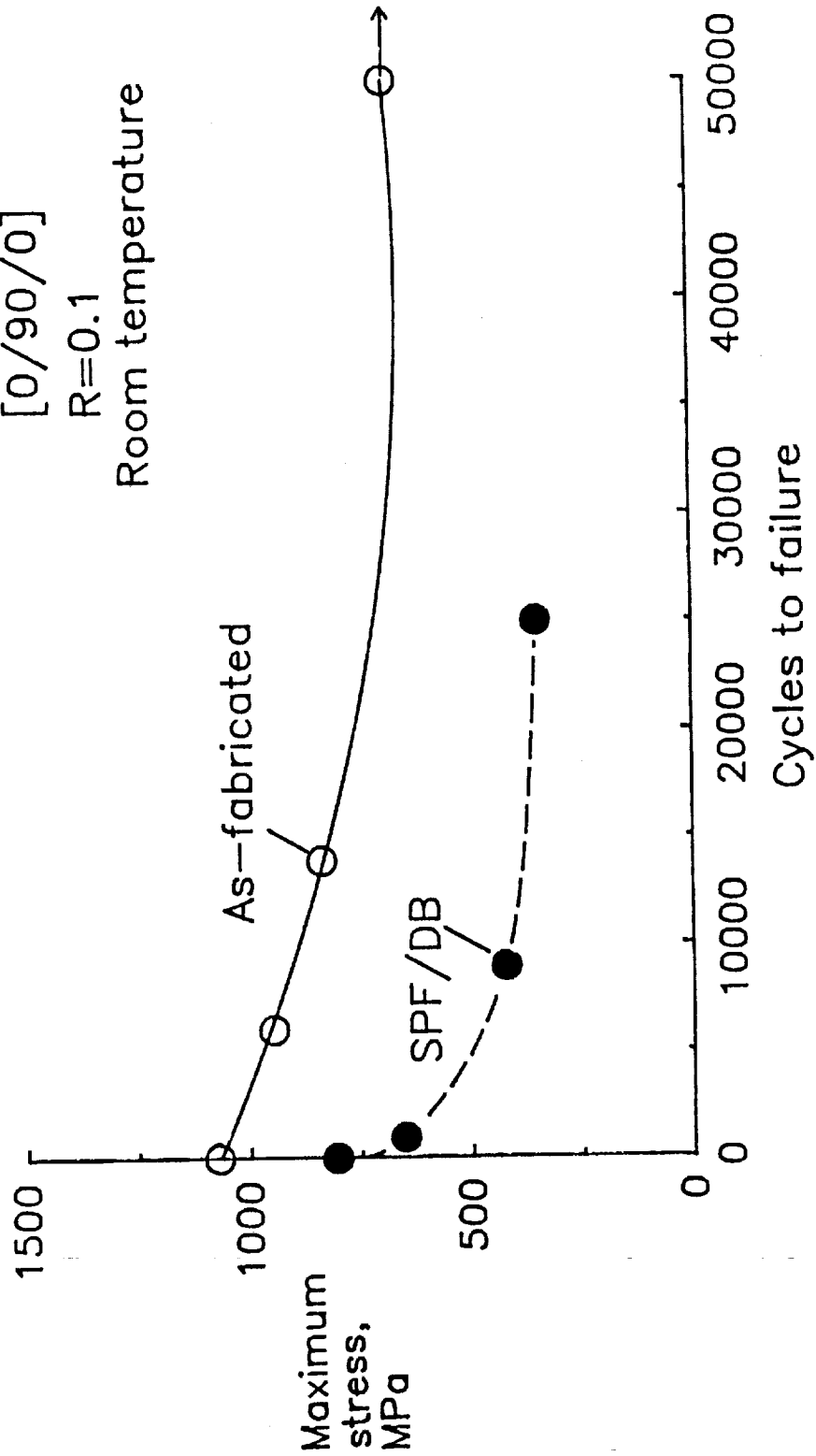
Figure 3.- S-N curves for ASF and SPF/DB [0/90/0] SCS-6/Ti-15-3

laminates [2].

SPF/DB

ASF

Fiber failure behind
crack tip
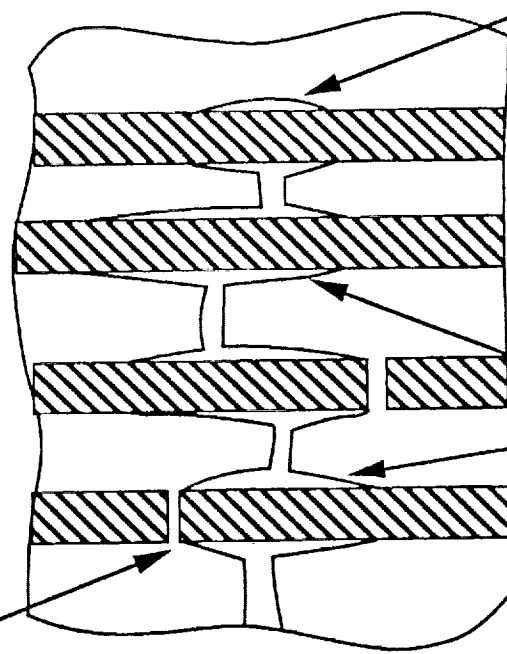
Crack-tip
blunting

Fiber/matrix
debonding
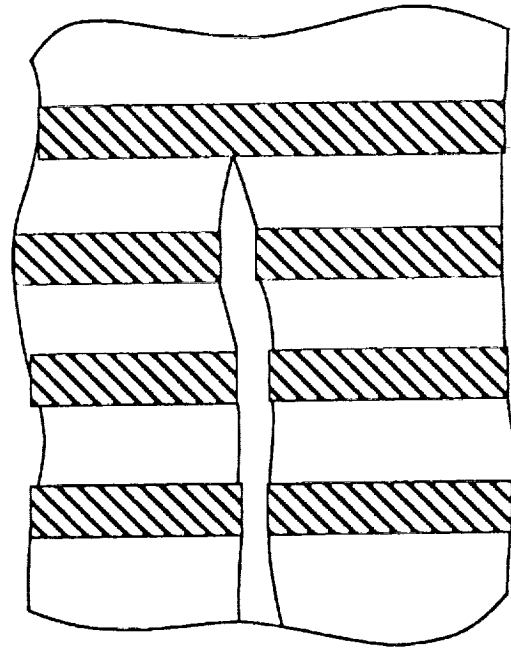
Figure 4.- Failure mechanisms in 0° ply for ASF and SPF/DB [0/90/0]

laminates [2].

24

SCS-6/Ti-15-3

6.35 DIA

70 · 19 · 9.5 · 70

(b) Center-hole specimen

Not to scale

All dimensions in mm

70 · 19 · 0.45 · 3 · 70

(a) Edge-notched specimen

Figure 5.- Specimen configuration and dimensions.

25
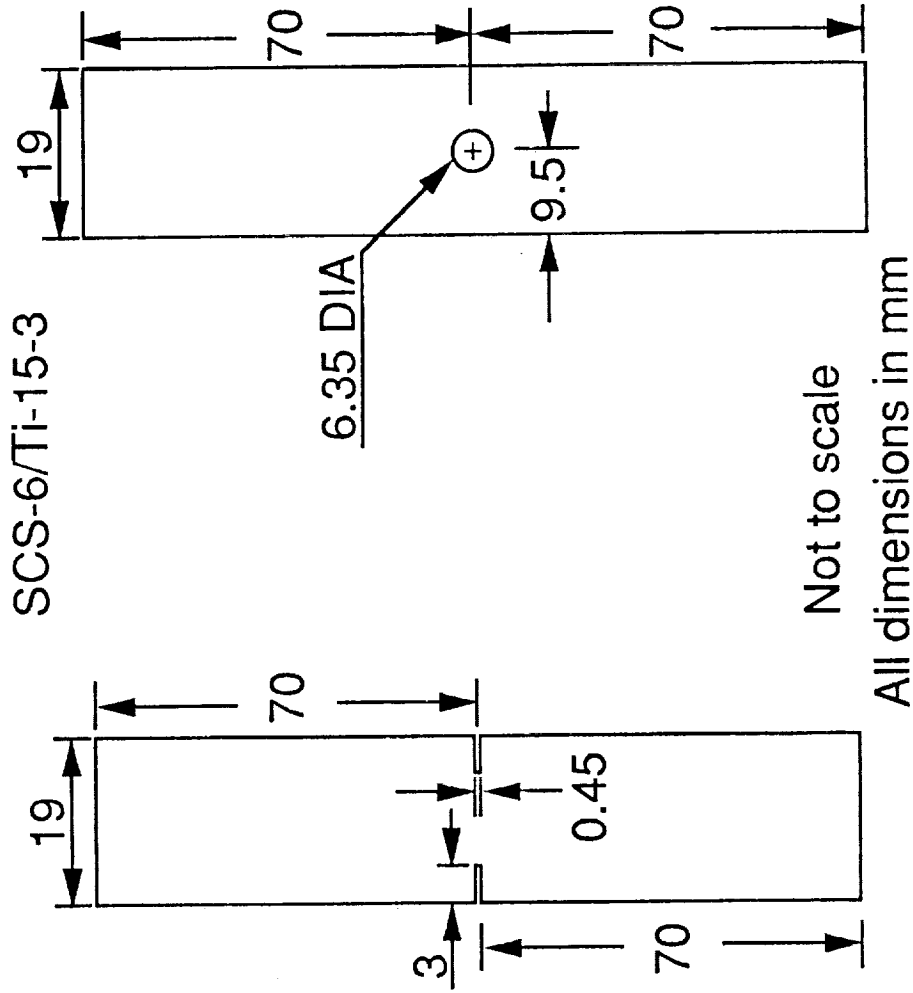
SCS-6/Ti-15-3
[0/90/0]

Center-Hole Specimen
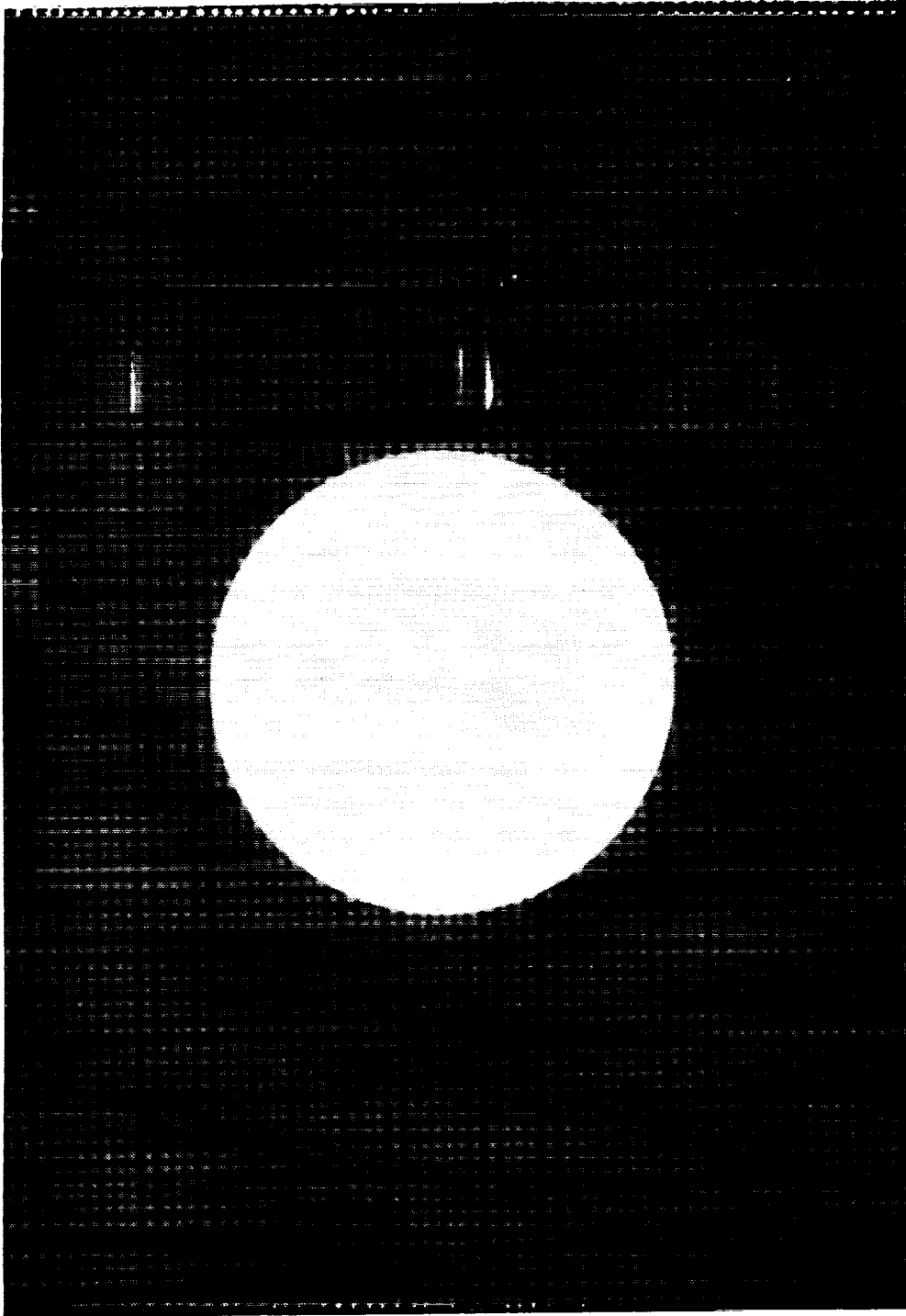
Figure 6.- Radiograph of SCS-6/Ti-15-3 [0/90/0] center-hole specimen.

SCS-6/Ti-15-3
[0]$_8$
As-fabricated
Stress ratio = 0.1
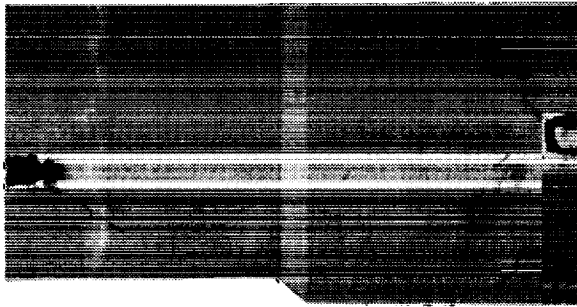
(a) Max. stress = 280 MPa;
50,000 cycles

(b) Max. stress = 310 MPa;
50,000 cycles

**Double edge
notched specimen**

⌐──────┐
1 mm
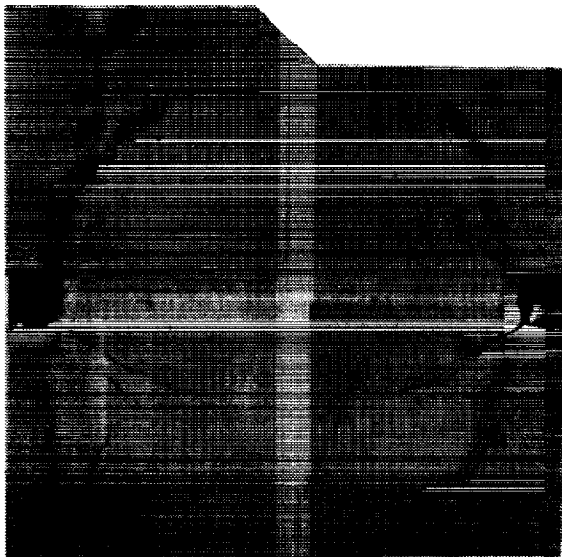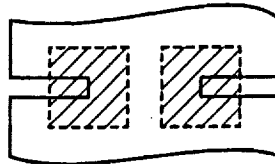
(c) Max. stress = 345 MPa;
50,000 cycles

(d) Max. stress = 380 MPa;
50,000 cycles

Figure 7.- Surface replicas of damage growth in ASF [0]$_8$ specimen.

27

SCS-6/Ti-15-3
[0]₈
As-fabricated
Stress ratio = 0.1

Double edge
notched specimen

Surface replica at
50,000 cycles and
290 MPa max. stress

Surface replica at
50,000 cycles and
290 MPa max. stress

1 mm
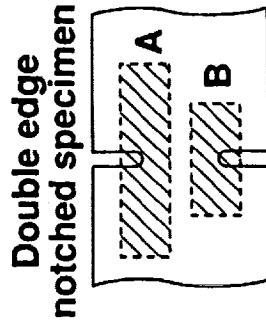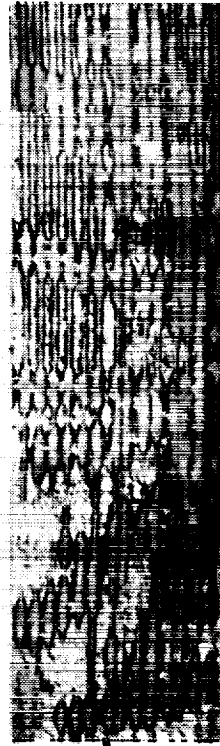
Etched surface
layer showing
fibers underneath

Figure 8.- Surface replicas and etched surface layer for ASF [0]₈
specimen.

28

SCS-6/Ti-15-3
[0]₈ Aged
Max. stress = 250 MPa
Stress ratio = 0.1

Double edge
notched specimen
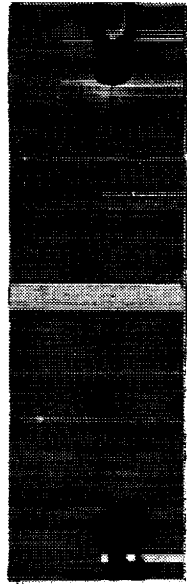
(a) After 15,000 cycles
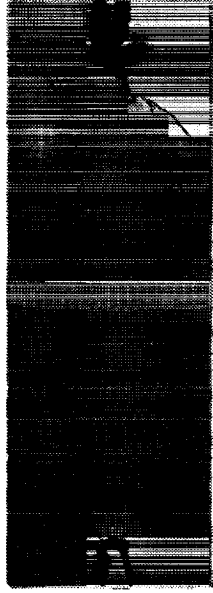
(b) After 75,000 cycles

(c) After 200,000 cycles

(d) After 550,000 cycles

1 mm

Figure 9.- Surface replicas of damage growth in aged [0]₈ specimen.

Double edge notched specimen
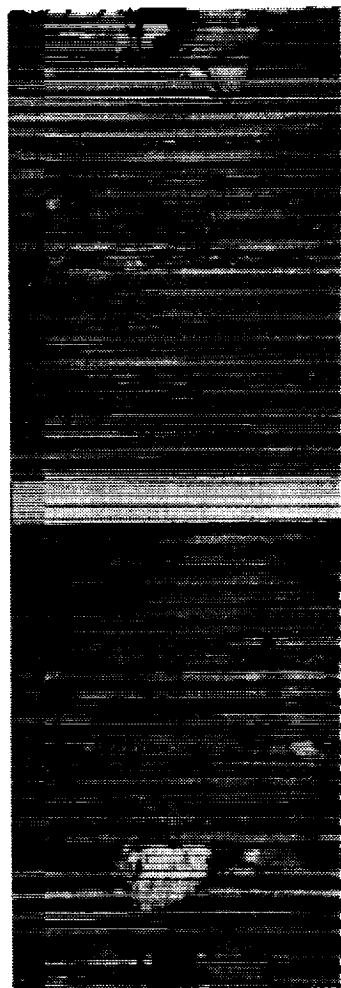
SCS-6/Ti-15-3 [0]$_8$
Aged
Stress ratio = 0.1

⊢ 1 mm
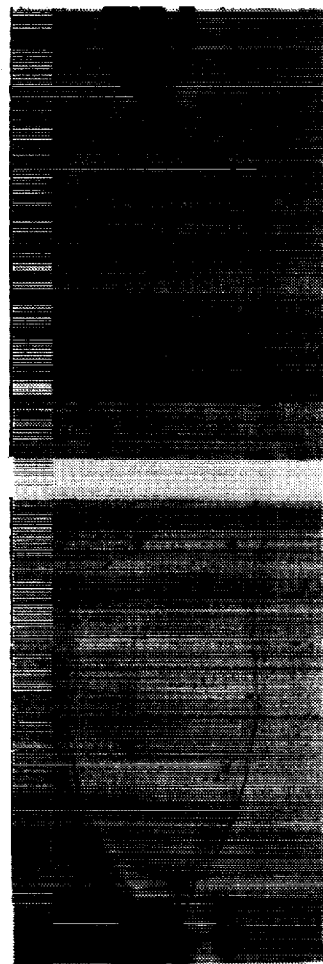
(a) Surface replica at 700,000 cycles
(max. stress = 250 MPa)

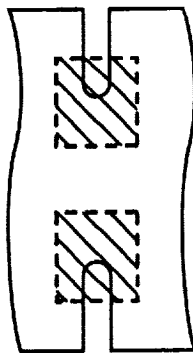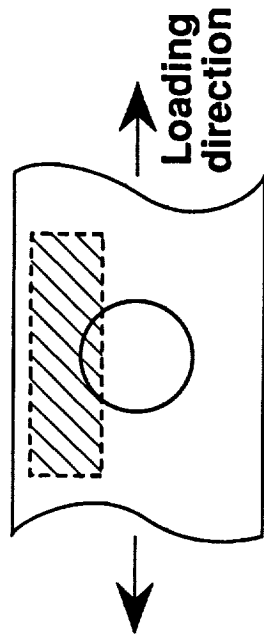(b) Etched surface layer showing fibers underneath

Figure 10.- Surface replicas and etched surface layer for aged [0]$_8$
specimen.

SCS-6/Ti-15-3
[0/90]$_{2s}$
As-fabricated

Max. stress = 150 MPa
50,000 cycles
R = 0.1

⊢————⊣ 1 mm

Loading
direction

Figure 11.- Surface damage for center hole ASF [0/90]$_{2s}$ specimen.

Center hole specimen

SCS-6/Ti-15-3
[0/90]$_{2s}$
As-fabricated
Max. stress = 150 MPa
50,000 cycles
R = 0.1

Loading direction

Edge of hole

Matrix

Fiber

25 µm

(a) Matrix cracking

Debonded area

Fiber

Matrix

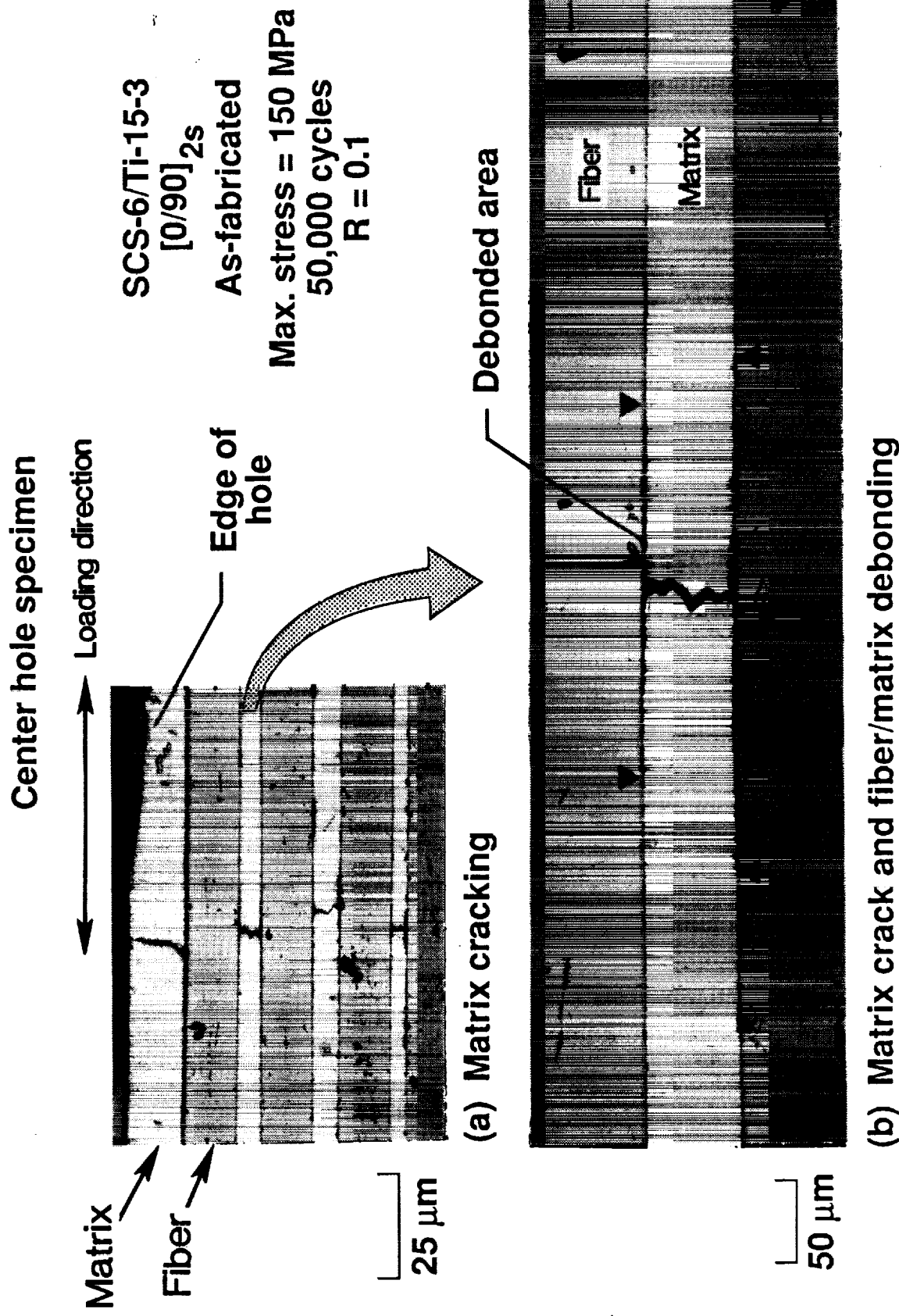50 µm

(b) Matrix crack and fiber/matrix debonding

Figure 12.- Damage in 0 degree ply of [0/90]$_{2s}$ ASF specimen with center hole.

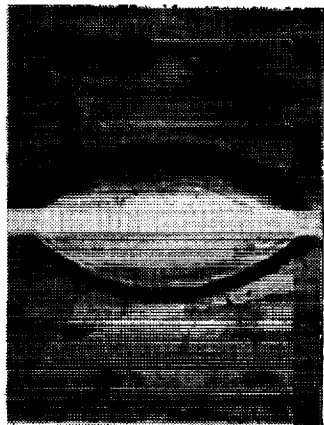SCS-6/Ti-15-3   [0/90/0]
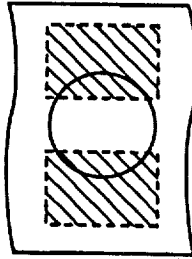As-fabricated

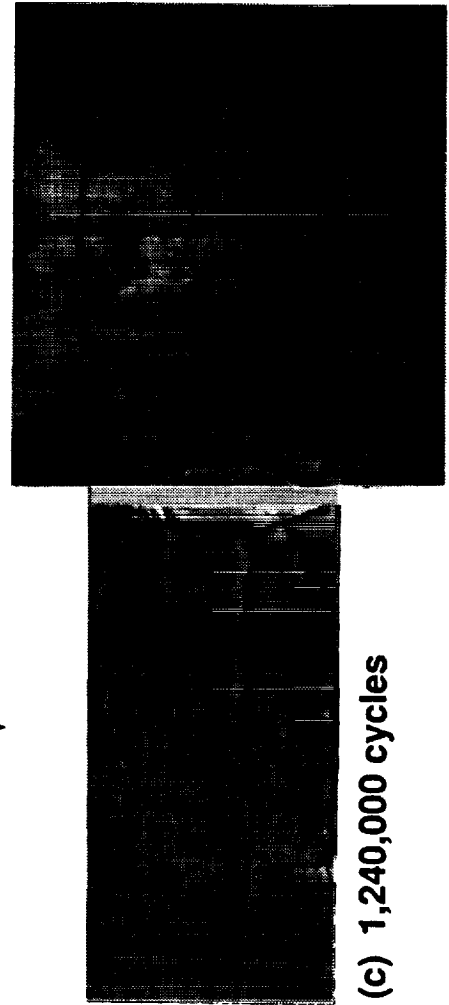Max. stress = 215 MPa
Stress ratio = 0.1

1 mm

(b) 500,000 cycles

Open hole specimen

Loading direction

(a) 100,000 cycles

(c) 1,240,000 cycles

Figure 13.- Surface replicas of damage growth in [0/90/0] ASF specimen.

33

SCS-6/Ti-15-3
[0/90/0]
SPF/DB
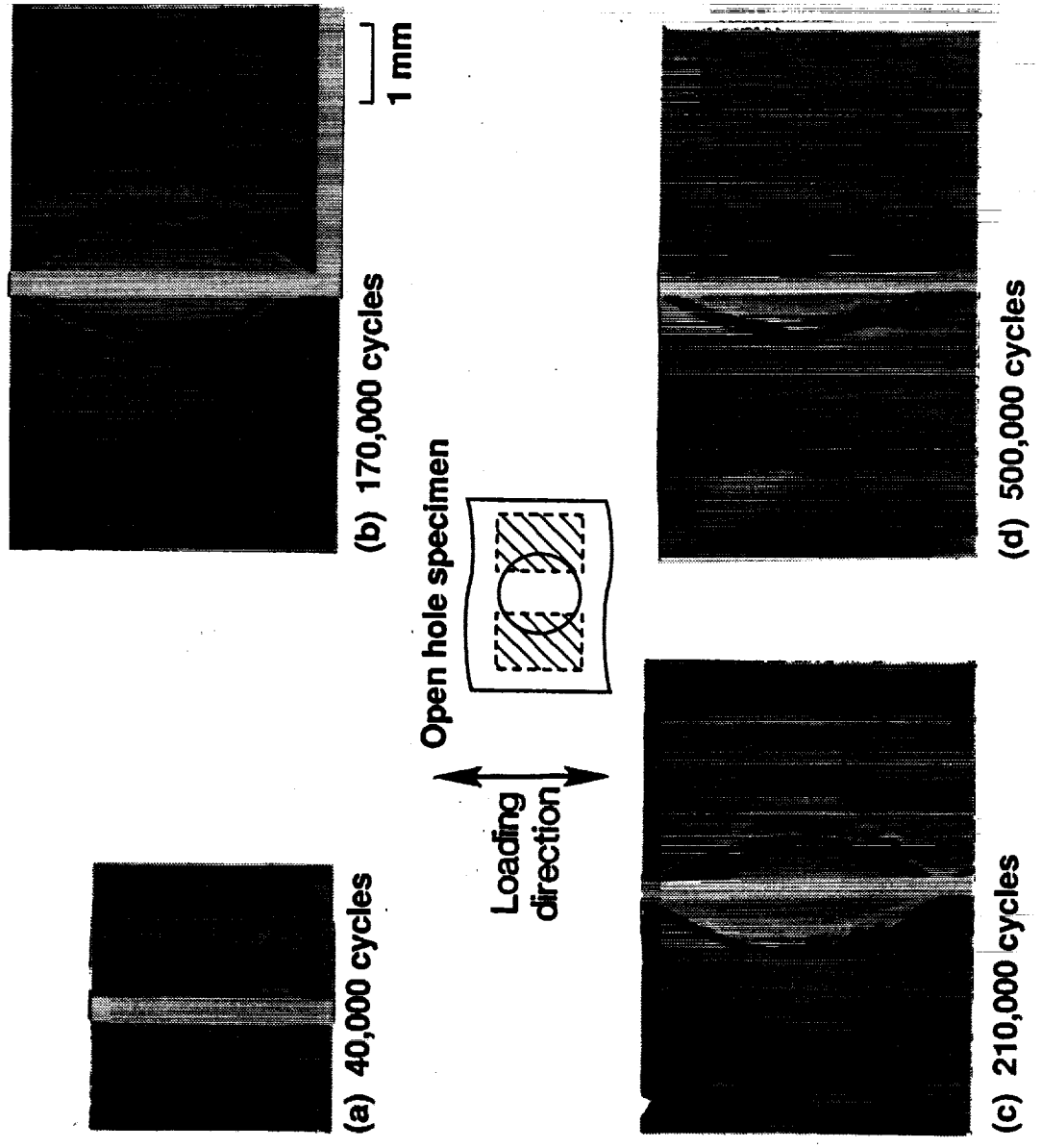
Max. stress = 215 MPa
Stress ratio = 0.1

(a) 40,000 cycles

(b) 170,000 cycles

1 mm

Open hole specimen

Loading direction

(c) 210,000 cycles

(d) 500,000 cycles

Figure 14.- Surface replicas of damage growth in [0/90/0] SPF/DB specimen.

34

NASA

National Aeronautics and
Space Administration

Report Documentation Page

1. Report No.	2. Government Accession No.	3. Recipient's Catalog No.
NASA TM-101688		

4. Title and Subtitle	5. Report Date
Observations of Fatigue Crack Initiation and Damage Growth in Notched Titanium Matrix Composites	January 1990
	6. Performing Organization Code

7. Author(s)	8. Performing Organization Report No.
R. A. Naik* and W. S. Johnson	
	10. Work Unit No.
	505-63-01-05

9. Performing Organization Name and Address	11. Contract or Grant No.
NASA Langley Research Center Hampton, VA 23665-5225	
	13. Type of Report and Period Covered

12. Sponsoring Agency Name and Address	
National Aeronautics and Space Administration Washington, DC 20546	Technical Memorandum
	14. Sponsoring Agency Code

15. Supplementary Notes

16. Abstract

The purpose of this study was to characterize damage initiation and growth in notched titanium matrix composites at room temperature. Double edge notched or center open hole SCS-6/Ti-15-3 specimens containing 0° plies or containing both 0° and 90° plies were fatigued. The specimens were tested in the as-fabricated (ASF) and in heat-treated conditions. A local strain criterion using unnotched specimen fatigue data was successful in predicting fatigue damage initiation. The initiation stress level was accurately predicted for both a double edge notched unidirectional specimen and a cross-plied center hole specimen. The fatigue produced long multiple cracks growing from the notches. These fatigue cracks were only in the matrix material and did not break the fibers in their path. The combination of matrix cracking and fiber/matrix debonding appears to greatly reduce the stress concentration around the notches. The laminates that were heat treated showed a different crack growth pattern. In the ASF specimens, matrix cracks had a more tortuous path and showed considerable more crack branching. For the same specimen geometry and cyclic stress, the [0/90/0] laminate with a hole had far superior fatigue resistance than the matrix only specimen with a hole.

17. Key Words (Suggested by Author(s))	18. Distribution Statement
Metal matrix composite silicon carbide fibers fiber/matrix interface	Unclassified - Unlimited Subject Category - 24

19. Security Classif. (of this report)	20. Security Classif. (of this page)	21. No. of pages	22. Price
Unclassified	Unclassified	35	A03

NASA FORM 1626 OCT 86